Mon. Not. R. Astron. Soc. **315**, 740–750 (2000)

Optical properties of the carbon dust grains in the envelopes around asymptotic giant branch stars

Kyung-Won Suh★

Department of Astronomy and Space Science, Chungbuk National University, Cheongju-City, 361-763, Republic of Korea

Accepted 2000 February 3. Received 1999 October 15; in original form 1999 July 5

ABSTRACT

We have investigated the optical properties of the carbon dust grains in the envelopes around carbon-rich asymptotic giant branch stars, paying close attention to the infrared observations of the stars and the laboratory-measured optical data of the candidate dust grain materials. We have compared the radiative transfer model results with the observed spectral energy distributions of the stars including *IRAS* Point Source Catalog and *IRAS* Low Resolution Spectrograph data. We have deduced an opacity function of amorphous carbon dust grains from model fitting with infrared carbon stars. From the opacity function, we have derived the optical constants of the AMC grains. The optical constants satisfy the Kramers–Kronig relation and produce the opacity function that fits the observations of infrared carbon stars better than previous works in the wide wavelength range 1–1000 μm. We have used simple mixtures of the AMC and silicon carbide grains for modelling. We have compared the contributions that AMC and SiC grains make to the opacity for the cases of simple mixtures of them and spherical core–mantle type grains consisting of a SiC core and an AMC mantle.

Key words: radiative transfer – stars: AGB and post-AGB – circumstellar matter – dust, extinction – infrared: stars.

1 INTRODUCTION

Infrared observations of carbon-rich asymptotic giant branch (AGB) stars have revealed some types of carbon dust grains in the envelopes around them. They are amorphous carbon (AMC), silicon carbide (SiC) and magnesium sulfide (MgS). The main site of dust formation is believed to be the cool envelopes around AGB stars. The carbon dust grains may go through some physical and chemical changes after they are blown away from the AGB stars. Therefore, the opacity functions of the carbon dust grains in AGB stars are probably different from those obtained from interstellar dust grains and laboratory measurements of terrestrial or meteoritic materials. The determination of the optical properties of carbon dust grains in the envelopes around AGB stars should be primarily based on the observations of the stars as well as the appropriate physical constraints.

Carbon stars are generally believed to be the evolutionary successors of M-type Mira variables that have thin oxygen-rich dust envelopes. When AGB stars of intermediate mass range go through carbon 'dredge-up' processes, and thus the abundance of carbon is larger than that of oxygen, oxygen-rich dust grain formation ceases and the stars become visual carbon stars. After that phase, carbon-rich dust grains start forming and the stars evolve into infrared carbon stars with thick carbon-rich dust envelopes and very high mass loss rates (Iben 1981; Chan & Kwok 1990; Groenewegen, van den Hoek & de Jong 1995).

AMC dust grains play a major role in producing the overall shape of the spectral energy distributions (SEDs) of carbon-rich AGB stars in the wavelength range 1–1000 μm. Based on laboratory measurements of AMC, Rouleau & Martin (1991) and Zubko et al. (1996) have obtained the optical constants that are consistent with physical constraints, but without verifying that the radiative transfer model fitted satisfactorily with the observations of AGB stars.

Using the optical constants of AMC from Rouleau & Martin (1991), a number of authors (Lorenz-Martins & Lefèvre 1994; Blanco et al. 1998; Groenewegen et al. 1998) modelled carbon-rich AGB stars. However, their radiative transfer model results did not satisfactorily fit with the observations of a wide sample of objects in the wide wavelength range 1–1000 μm. On the other hand, Rowan-Robinson & Harris (1983), Chan & Kwok (1990), Le Bertre (1997) and Suh (1997) empirically obtained the opacity functions that fitted the observations of infrared carbon stars well without verifying whether the dielectric function so obtained was consistent with the Kramers–Kronig dispersion relation.

In this paper, we investigate the optical properties of the carbon dust grains in the envelopes around AGB stars, paying close attention to the observations of the stars as well as the appropriate

★ E-mail: kwsuh@cbucc.chungbuk.ac.kr

physical constraints. We compare the radiative transfer model results with the observed SEDs of the stars taken from the *IRAS* Point Source Catalog (PSC, Joint *IRAS* Science Working Group 1986b) and the *IRAS* Low Resolution Spectrograph (LRS, Joint IRAS Science Working Group 1986a) data. We present the optical constants of the AMC grains in the envelopes around carbon-rich AGB stars. The optical constants satisfy the Kramers–Kronig relation and produce an opacity function that fits the observations of infrared carbon stars better than in previous works. When we mix SiC grains with the AMC grains the model results fit observed SEDs in the wide wavelength range 1–1000 μm fairly well. The aim and procedure of this paper are similar to those of Suh (1999, hereafter Paper I) except that the main subject of paper I is the silicate dust grains in the envelopes around oxygen-rich AGB stars.

2 CARBON DUST OPACITY

Rowan-Robinson & Harris (1983) reproduced large-sample SEDs of carbon stars with AMC adopting the absorption efficiency law, $Q_{\rm abs} \propto \lambda^{-1}$. Recently, many authors have modelled carbon stars with AMC and SiC. Chan & Kwok (1990) used the empirical opacity function of SiC. This opacity pattern resembles the one for a mixture of AMC and a small amount of SiC. Lorenz-Martins & Lefèvre (1994) and Groenewegen et al. (1998) modelled infrared carbon stars with the opacity functions of both SiC and AMC. It was suggested that for AGB stars the 30-μm band could be produced by a small amount of MgS particles (Begemann et al. 1994; Omont et al. 1995). SiC and MgS dust grains have only a minor effect on the overall opacity of the dust grains in infrared carbon stars except for the small 11-μm SiC and 30-μm MgS features. However, optical constants of MgS have not been measured at visible and near-infrared wavelengths. Unlike the well-observed 11-μm SiC feature, only a number of objects were observed in the 30-μm band. In this paper, we use AMC and SiC dust grains for carbon dust opacity.

For given characteristics of the dust grain material (optical constants, size and shape) the absorption and scattering efficiency factors can be calculated at any given wavelength (e.g. Bohren & Huffman 1983). After many trials, we have found an opacity function of AMC grains that fit the observations better, but does not stray too far from the known characteristics of the materials. Using the deduced opacity we may derive the complex dielectric function $\varepsilon(\lambda) = \varepsilon_1 + {\rm i}\varepsilon_2$ when we consider further physical constraints: a dispersion model given by Clausius–Mosotti law for dielectrics or Kramers–Kronig relations (Bohren & Huffman 1983). The complex dielectric function may be expressed by the complex index of refraction $m(\lambda) = n + {\rm i}k$, where $\varepsilon = m^2$.

2.1 Deriving the optical constants for a new opacity function of AMC

As we will discuss in the next section, we find that the opacity function of AMC grains determines the quality of the overall fitting with observed SEDs of carbon-rich AGB stars in the wavelength range 1–1000 μm. We have deduced an opacity function of AMC dust grains from model fitting with infrared carbon stars. We will explain the radiative transfer models that are compared with the observations of AGB stars in the next sections. Fig. 1 shows the opacity function of AMC grains deduced in this paper and other functions that are obtained from the optical

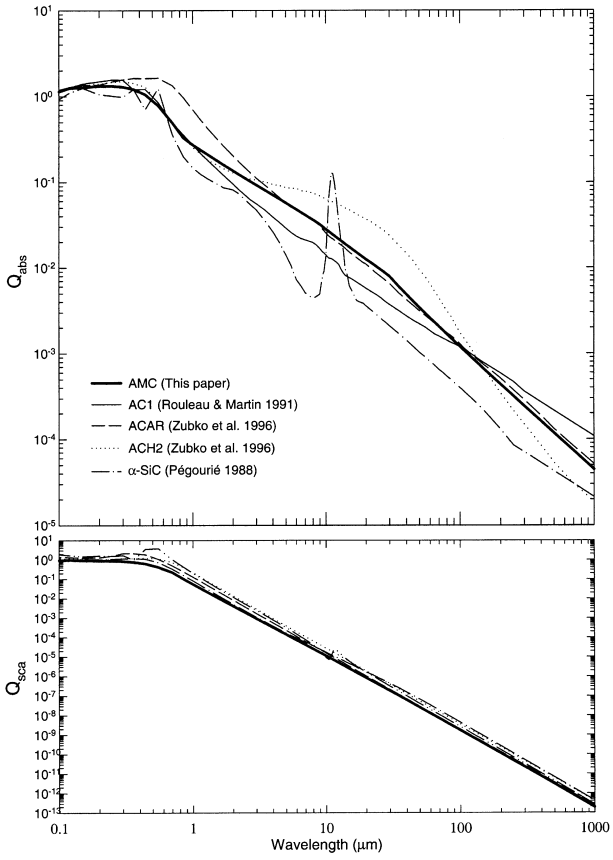

Figure 1. The opacity functions for carbon dust grains.

constants listed in Rouleau & Martin (1991) and Zubko et al. (1996). The opacity function of α SiC, obtained from the optical constants listed in Pégourié (1988), is also displayed. The absorption and scattering efficiency factors ($Q_{\rm abs}$ and $Q_{\rm sca}$) are calculated for a spherical dust grain with a radius of 0.1 μm. Note that other authors may have used different shapes and sizes of the dust grains in deriving the optical constants but that in this paper, we use spherical dust grains with uniform radii of 0.1 μm.

The opacity function of AMC grains deduced in this paper in a given wavelength region approximately matches the curve of a simple power law ($Q_{\rm abs} \propto \lambda^{-\beta}$), with a different spectral index β in each wavelength region. For $\lambda = 0.9$–$9\,\mu{\rm m}$, $\beta \sim 1$. For $\lambda =$ 9–30 μm, the function becomes steeper with $\beta \sim 1.2$ and for $\lambda =$ 30–1000 μm, the function becomes even steeper with $\beta \sim 1.5$. After many trials of comparison, we find that this opacity function fits the observations better than any other power-law opacity function with a single index in a wide wavelength region. The opacity functions of AMC grains measured by many authors in the laboratory show that the overall index takes various values ($\beta \sim 0.6$–1.5) depending on the degree and structure of crystallization of the AMC grains (Koike, Hasegawa & Manabe 1980; Borghesi, Bussoletti & Colangeli 1985; Bussoletti et al. 1987; Koike et al. 1995).

Derivation of two functions of complex dielectric constants, $\varepsilon_1(\lambda)$ and $\varepsilon_2(\lambda)$, from the deduced function $Q_{\rm ext}(\lambda)$ requires additional information. The supplementary physical constraint that the dielectric constants should satisfy is the Kramers–Kronig relation (Bohren & Huffman 1983). We have used the same procedure as used in Paper I to obtain the complex dielectric functions.

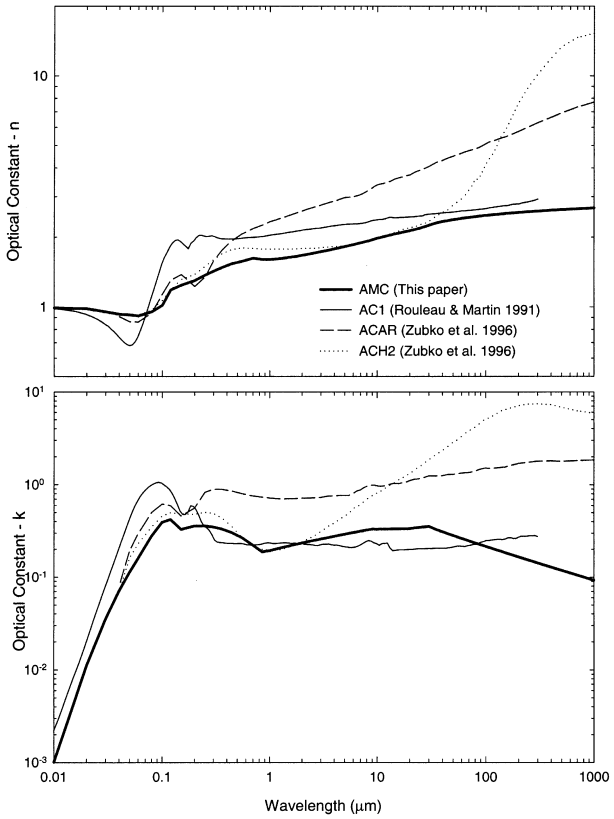

Figure 2. Complex optical constants for amorphous carbon dust grains.

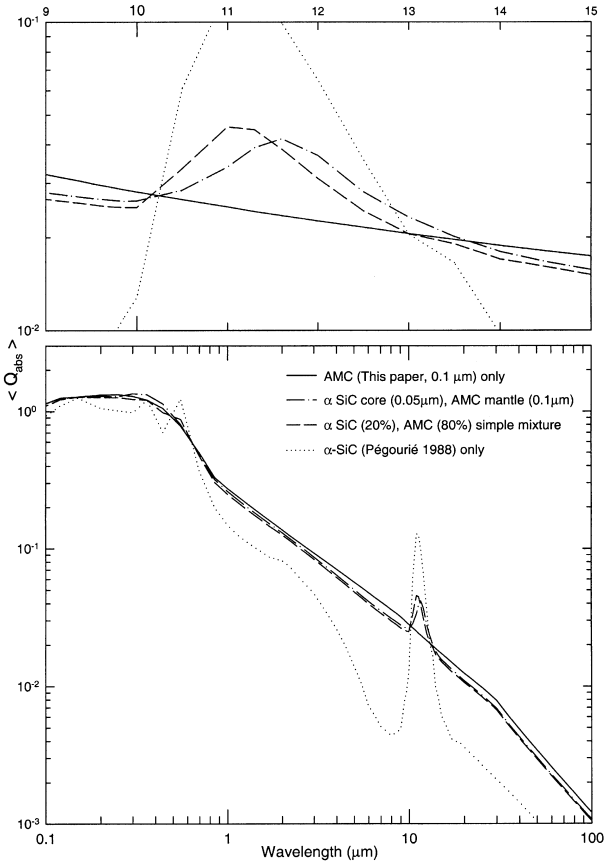

Figure 3. The average absorption efficiency factors for spherical core–mantle type grains and various mixtures of AMC and SiC grains.

From the satisfactory sets of complex dielectric constants we find the optical constants [$m(\lambda) = n + ik$]. In Fig. 2, we compare the optical constants derived for this paper with the values derived by other authors from laboratory measured optical data (Rouleau & Martin 1991; Zubko et al. 1996). Note that the optical properties are strongly dependent on shape, size and crystallization state of the grain materials (e.g. Koike et al. 1995). We have used spherical dust grains with uniform radii of 0.1 μm in deriving the optical constants. However, Rouleau & Martin (1991) and Zubko et al. (1996) used ellipsoidal form of grains in deriving the optical constants. The two sets of the optical constants derived in this paper satisfy the Kramers–Kronig relation and produce the opacity function that fits the observations of AGB stars better than in previous works as we will discuss later.

2.2 SiC grains

Lorenz-Martins & Lefèvre (1994) and Groenewegen (1995) suggested that the ratio of SiC to AMC grains decreases as the total optical depth increases, or as infrared carbon stars evolve. The SiC emission feature is either very weak or does not exist in the spectra of extreme infrared carbon stars with optically thick dust envelopes (e.g. Kozasa et al. 1996). Lorenz-Martins & Lefèvre (1994) suggested the dust condensation temperature of SiC is hotter than that of AMC. Kozasa et al. (1996) suggested that SiC cores are formed at higher temperatures and AMC mantles are formed later in the outer region of the dust envelope.

Borghesi et al. (1985) measured the absorption spectra of the powder samples of hexagonal form α SiC and cubic form β SiC. Pégourié (1988) derived the optical constants of α SiC. Groenewegen (1995), Speck, Barlow & Skinner (1997), Blanco et al. (1998) argued that most of the SiC features of carbon stars can be fitted with the α SiC grains. This looks to be unreasonable because β SiC is the form most commonly found in meteorites. Speck, Hoffmeister & Barlow (1999) pointed out that the discrepancy can be removed when we use the correct KBr matrix method. Namely, in the process of correcting the laboratory measured spectra, significant errors can be involved.

In Fig. 3 we compare the contributions that AMC and SiC grains make to the opacity (the average absorption efficiency factors; $\langle Q_{\rm abs} \rangle$) of a simple mixture of spherical, same sized (0.1 μm) AMC, SiC and core–mantle type grains (that consist of an SiC core and an AMC mantle). We have used the optical constants of α SiC from Pégourié (1988) and the derived optical constants of AMC from this paper. Even for the same combination of materials, the spectral shapes are different. For the core–mantle type grains, the absorption peak of the SiC feature shifts to a longer wavelength.

For the case of a simple mixture, we find that the opacity using α SiC grains from Pégourié (1988) fits carbon-rich AGB stars fairly well. Previous authors used similar mixtures to reproduce the SiC features, as mentioned earlier. According to Borghesi et al. (1985), β SiC grains show the 11-μm absorption peak at a shorter wavelength. Even if the optical constants of β SiC are unavailable for testing, we can expect that fitting with β SiC could be as good as fitting with α SiC when we use core–mantle type grains because of the shift of the SiC peak. This could be another concern in investigating the ratio of α SiC to β SiC.

Table 1. Some characteristic parameters used by a number of authors for modelling carbon-rich AGB stars.

Auth.	AMC dust	SiC dust	T_c	Grain size	Central star
S	[a]This paper	[a]Pégourié (1988)	$T_c = 1000$ K	0.1 μm	$T_* = 2000$ K
B98	[b]Bussoliti et al. (1987)	[b]Borghesi et al. (1985)	variable $T_c < 1500$ K	0.008–0.04 μm	$T_* = 1300$–2950 K
G98	[a]Rouleau & Martin (1991)	[a] Pégourié (1988)	variable $T_c = 600$–1500 K	0.1 μm (model A)	$T_* = 2500$–3000 K
L97	$Q_{abs} \propto \lambda^{-1.3}$	–	$T_c = 950$ K	–	$T_* = 2200$–2600 K
S97	$Q_{abs} \propto \lambda^{-1}$	–	$T_c = 1000$ K	0.1 μm	$T_* = 2000$ K
L94	[a]Rouleau & Martin (1991)	[a]Pégourié (1988)	variable $T_c = 900$–1200 K	0.04–0.1 μm	$T_* = 1900$–2700 K
C90	–	synthesized Q_{abs}	$T_c = 1500$ K	–	$T_* = 2250$ K

Notes: Auth. – S, this paper; B98, Blanco et al. (1998); G98, Groenewegen et al. (1998); L97, Le Bertre (1997); S97, Suh (1997); L94, Lorenz-Martins & Lefèvre (1994); C90, Chan & Kwok (1990).
[a] The optical constants from the reference are used.
[b] The extinction curves from the reference are used.

3 DUST ENVELOPE MODEL CALCULATIONS

For this paper, we have used the radiative transfer code developed by Ivezic & Elitzur (1997) for a spherically symmetric dust shell. We have performed the model calculations in the wavelength range 0.01–36 000 μm. The wavelength dependence of the dust opacity is a fixed model parameter for the dust envelope, and was described in the previous section. Table 1 summarizes some characteristic parameters of model calculations for carbon-rich AGB stars performed by many authors.

3.1 Stellar parameters

For the central star, the luminosity is taken to be $10^4\,L_\odot$ and a stellar blackbody temperature (T_*) of 2000 K is used. A change in the luminosity does not affect the shape of the output spectra, it only affects the overall energy output. A change in the blackbody temperature of the central star does affect the output spectra.

3.2 Dust shell parameters

In this paper, to model the SEDs of infrared carbon stars we use simple mixtures of AMC and SiC grains for dust opacity. The opacity of the AMC grains determines the overall fitting in the wide wavelength region and SiC grains produce small but prominent 11-μm SiC features, which have been observed by *IRAS* LRS. We calculate the absorption and scattering efficiency factors using the optical constants of AMC grains derived in this paper and the optical constants of α SiC grains from Pégourié (1988). For all the models discussed in this paper, we use spherical dust grains with uniform radii of 0.1 μm except when specified otherwise.

We assume that the dust condensation temperature (T_c) is 1000 K for both AMC and SiC. The radius at which the dust temperature becomes T_c is taken to be the inner radius (R_c) of the dust shell. The outer radius of the dust shell is always taken to be 10 000 R_c. The adjustable input parameters are the dust optical depth at 10 μm (τ_{10}) and the radial dust density distribution. For this paper, we assume that the dust density distribution is continuous ($\rho \propto r^{-2}$). A detailed discussion of the dust density distribution can be found in Paper I. By fixing both the dust density distribution and the dust condensation temperature ($\rho \propto r^{-2}$ and $T_c = 1000$ K) for a wide sample of objects, we may have a better chance of finding the appropriate dust opacity.

Fig. 4 shows sample model results. The results show that SiC grains have only a minor effect on the overall SED, except for the small 11-μm SiC feature. We find that AMC dust grains play a major role in producing the overall shape of the SED in the wavelength region 1–1000 μm. Therefore, the opacity function of AMC determines the overall fitting to observed SEDs of carbon-rich AGB stars.

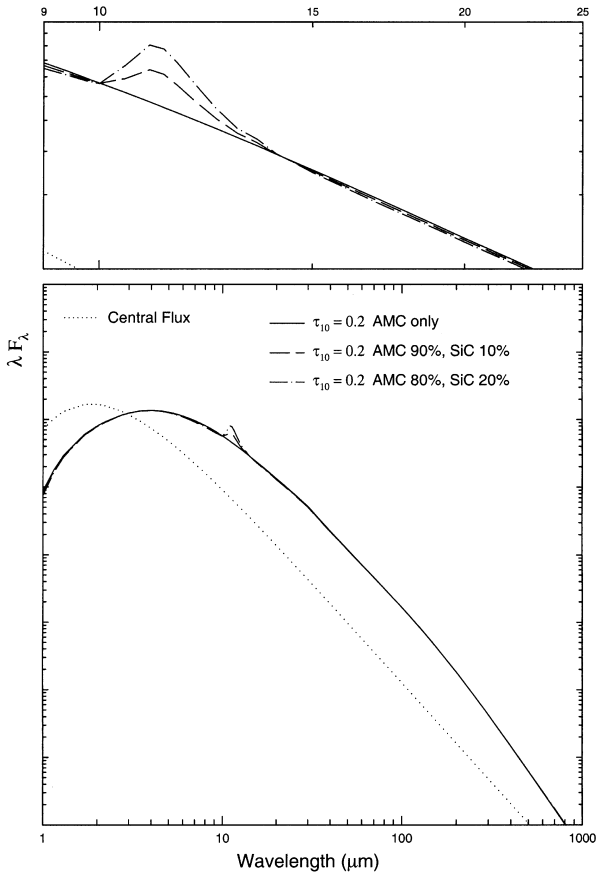

Figure 4. Model results with various mixtures of AMC and SiC grains.

4 SPECTRAL ENERGY DISTRIBUTION COMPARISON

In this section, we compare the observed SEDs for a selection of infrared carbon stars with model results. Most of the data for these stars are taken from the fourth edition of the Catalog of Infrared Observations (Gezari, Pitts & Schmitz 1998) and references therein.

Table 2. Twelve selected stars for SED comparison.

GCVS	*IRAS* PSC	AFGL	IRC	τ_{10}
R Lep	04573−1452	667	–	0.04
RU Vir	12447+0425	1579	00224	0.04
–	07270−1921	1131	−20131	0.06
R For	02270−2619	337	–	0.1
T Dra	17556+5813	2040	+60255	0.15
V1965 Cyg	19321+2757	2417	+30374	0.3
–	20570+2745	2686	–	0.5
LP And	23320+3416	3116	+40540	0.6
–	03186+7016	482	–	0.8
CW Leo	09452+1330	1381	+10216	0.8
–	23166+1655	3068	–	2.6
–	01144+6658	190	–	3

For modelling, we choose twelve infrared carbon stars covering a wide range in optical thickness of the dust shell as representatives of our results. The twelve stars were chosen because they have more complete observed SEDs covering a wider wavelength range than any other infrared carbon stars. As optical carbon stars may have oxygen-rich dust grains in their outer shells, we therefore only use infrared carbon stars for a valid sample. Table 2 lists the twelve selected stars and their best fitting optical depths. Results of the model calculations (lines) superimposed on the observational data (symbols) are shown in Figs 5 and 6 . In Fig. 5, the open symbols represent the observed SEDs and the filled symbols are scaled SEDs which we will describe later. The references for the observed data are listed in the figures. For all the stars, the *IRAS* LRS data and the *IRAS* PSC 4-colour photometric data are displayed. For each object, we show the SED comparison in the wide wavelength range from 1 (or 0.5) to 100 (or 1000) μm, depending on the data availability. A similar SED comparison in the narrower wavelength range (9–25 μm) is also displayed for a detailed view of the SED around the 11-μm SiC feature.

The observational data for different dates will show variations because the carbon-rich AGB stars are long period variables (Miras). The main parameter that changes significantly depending on the pulsation phase is the luminosity. However, a change in the central luminosity with fixed dust shell parameters does not affect the shape of the output SEDs, it only affects the overall energy output (Ivezic & Elitzur 1997). The parameter that shows minor variations is the best-fitting optical depth. This could be a result of dust formation and evaporation processes (e.g. Gauger, Gail & Sedlmayr 1990; Suh, Jones & Bowen 1990). A different optical depth produces different shapes of the output SEDs. For the carbon stars R For, the optical depth $\tau_{1\,\mu m}$ changes from 1 at minimum to 0.7 at maximum phase (Le Bertre 1988). For the more dusty carbon star GL 3068, the optical depth $\tau_{1\,\mu m}$ changes from 36 at minimum to 26 at maximum phase (Le Bertre, Gougeon & Le Sidaner 1995). The results show that overall energy output changes significantly depending on the pulsation phase, but that the shape of observed SEDs only changes slightly. Therefore, the scaling of the observed SEDs at different phases does not produce a perfectly correct synthetic SED, but it could be a valid approximation for the purpose of this paper.

When the observed SEDs at a given phase cover only a limited wavelength band, we have simply scaled the observed SEDs taken on different dates to produce similar results at one or more common wavelengths. The positions of the *IRAS* LRS data are not scaled. In Fig. 5, the scaled positions are marked by filled symbols and the original positions are marked by open symbols. This allows us to create a more complete SED than what would otherwise be possible with a single data set from a single date. More careful and technical recalibration methods are required if two sets of data do not have common wavelengths.

For all the twelve objects displayed in Fig. 5, the overall fitting is relatively good in the wavelength range 1–1000 μm. The fitting in the range $\lambda = 1$–5 μm is especially better than that of previous works. Our opacity function, which is steep in the range $\lambda =$ 30–1000 μm with the approximate power law index of 1.5, fits the observations well for all of the twelve stars. We use simple mixtures of AMC and SiC grains. The small 11-μm SiC features are fairly well fitted with our models of simple grain mixtures.

The four objects that have relatively thin ($\tau_{10} = 0.04$–0.1) dust shells displayed in the first four panels of Fig. 5 show prominent SiC features. They require a larger portion (20 per cent) of SiC dust grains. The next four objects in the intermediate optical depth range ($\tau_{10} = 0.15$–0.6) displayed in Fig. 5 show less prominent SiC features. The last four, most dusty objects ($\tau_{10} = 0.8$–3) displayed in Fig. 5 show vague or no SiC features. Note that the observed data of IRC+10216 by Sopka et al. (1985) were recalibrated for phase variation by Rengarajan et al. (1985) but that the observed data by Sopka et al. (1985) for AFGL 3068 was not recalibrated. Lorenz-Martins & Lefèvre (1994) and Groenewegen (1995) suggested that the ratio of SiC to AMC grains decreases as the total optical depth increases or as infrared carbon stars evolve. Again, we find that the ratio of SiC to AMC grains appears to decrease as the total optical depth increases.

In Fig. 6, we compare the model SEDs using various opacity functions of AMC (see Fig. 1) with the observations of IRC+10216. We find that the opacity function of AMC grains obtained in this paper fits the observations better than previous works in the wide spectral region ($\lambda = 1$–1000 μm). As all the opacity functions show different extinctions at 10 μm, the best fitting τ_{10} is different for different opacity functions. The opacity function obtained from the optical constants of Zubko et al. (1996) fits the observations fairly well in the wavelength range 2–1000 μm. However, it requires a less steep opacity function in the range $\lambda = 1$–10 μm to make a satisfactory fit in the wavelength range 1–2 μm.

However, the deviations in the short wavelength region 0.5–1 μm could not be avoided (see Figs 5 and 6) and previous investigators have also noted this. The shape of the resulting SEDs in the range $\lambda = 0.5$–1 μm depends sensitively on the grain sizes. However, using smaller grain sizes does not improve the fitting (Fig. 6) and other observational evidence indicates that the grain size should be ∼0.15 μm for IRC+10216 (Groenewegen 1997). A more probable reason could be that these stars show very large scale variations in the region $\lambda < 1$ μm, even in short intervals of time.

We find that the opacity function for this paper fits the observations better than that of previous works in the wavelength range 1–1000 μm. Note that we have used the same assumptions of $\rho \propto r^{-2}$, $T_c = 1000$ K and $T_* = 2000$ K for all the SED models presented in this paper including the models with other opacity functions. However, the original authors of the other opacity functions may not have used the same assumptions in deriving their optical constants.

5 TWO-COLOUR DIAGRAMS

Only a relatively small number of carbon-rich AGB stars have complete or nearly complete SEDs. A large number of stars have

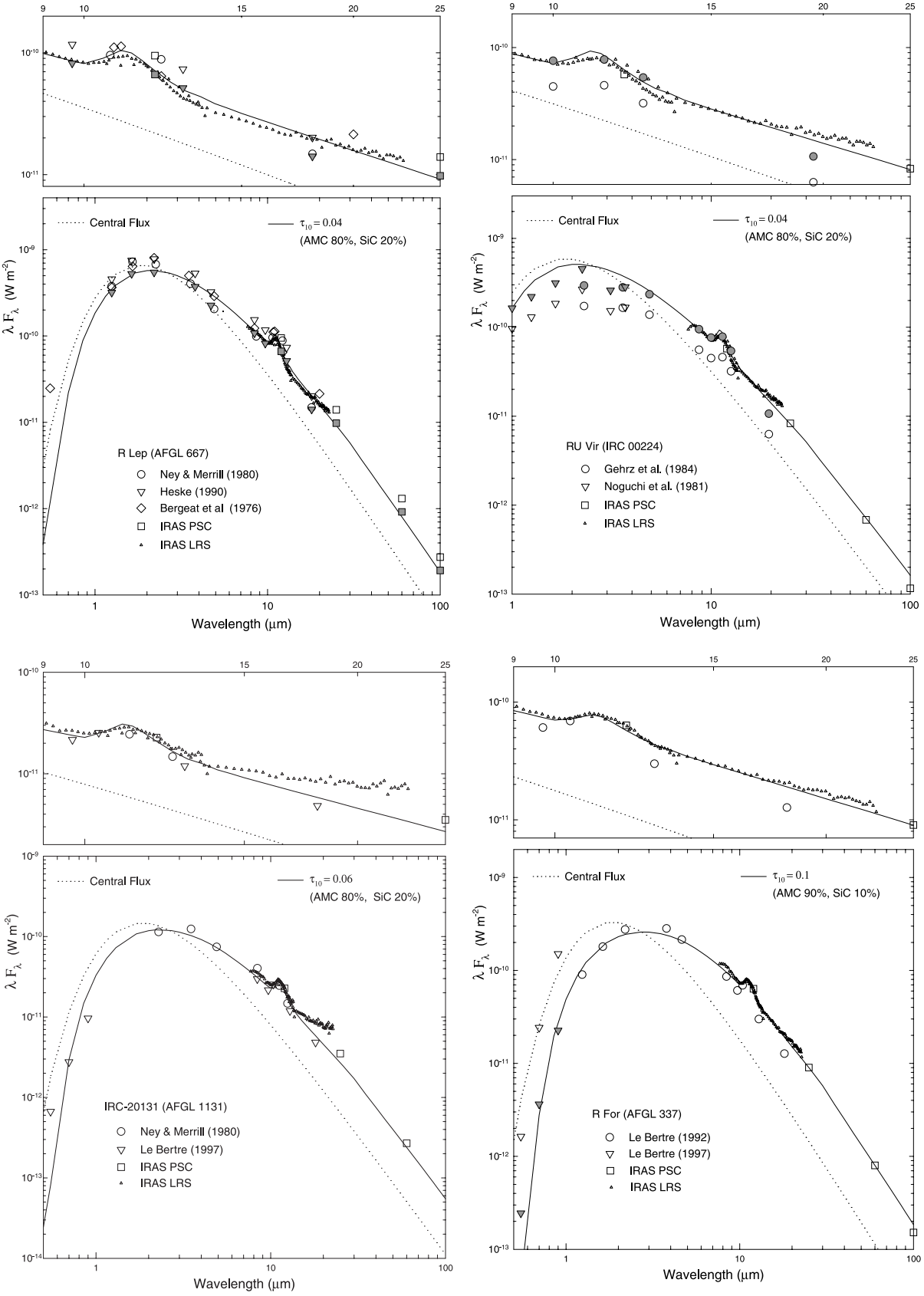

Figure 5. Model results compared with the observations for twelve stars.

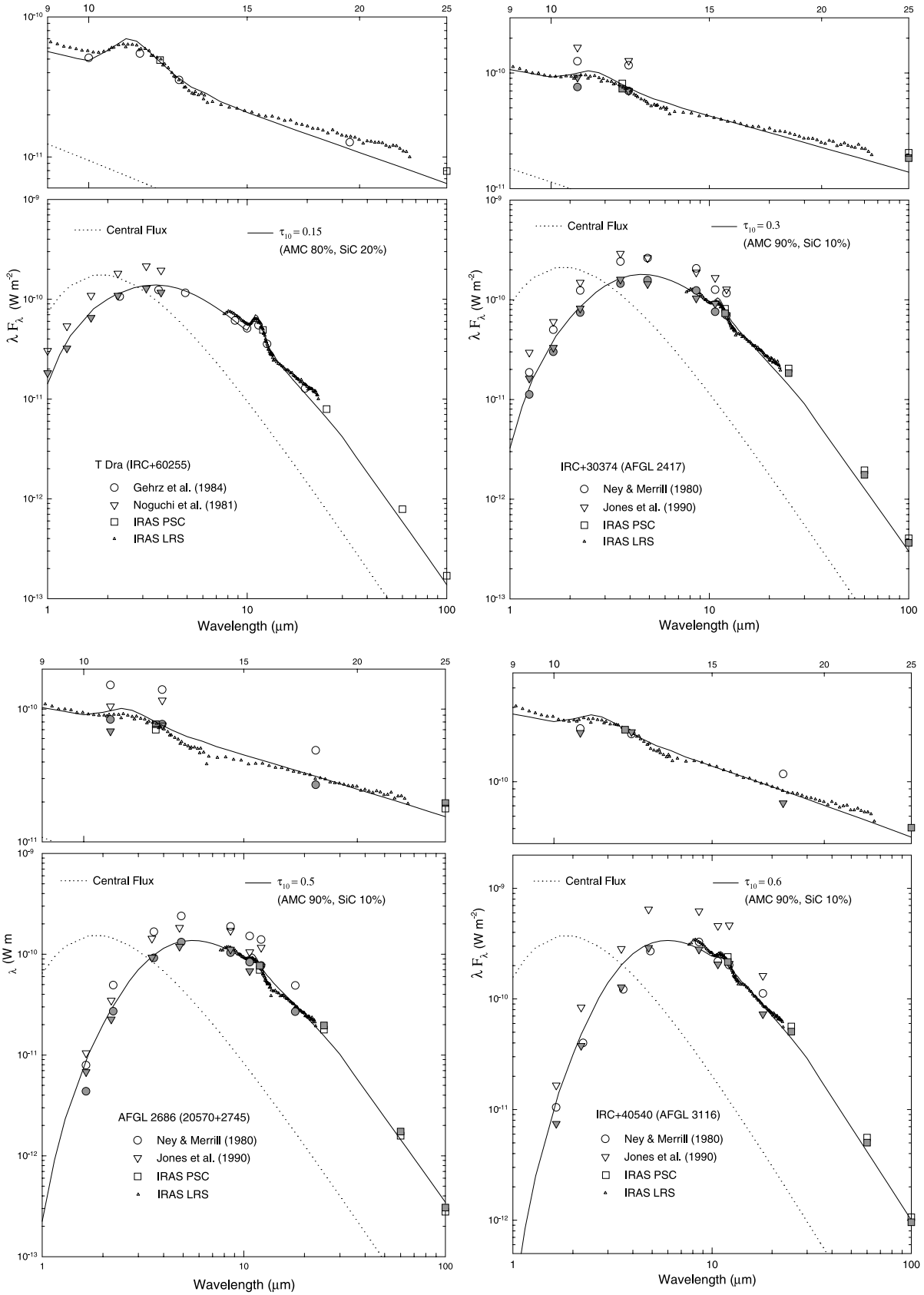

Figure 5 – *continued*

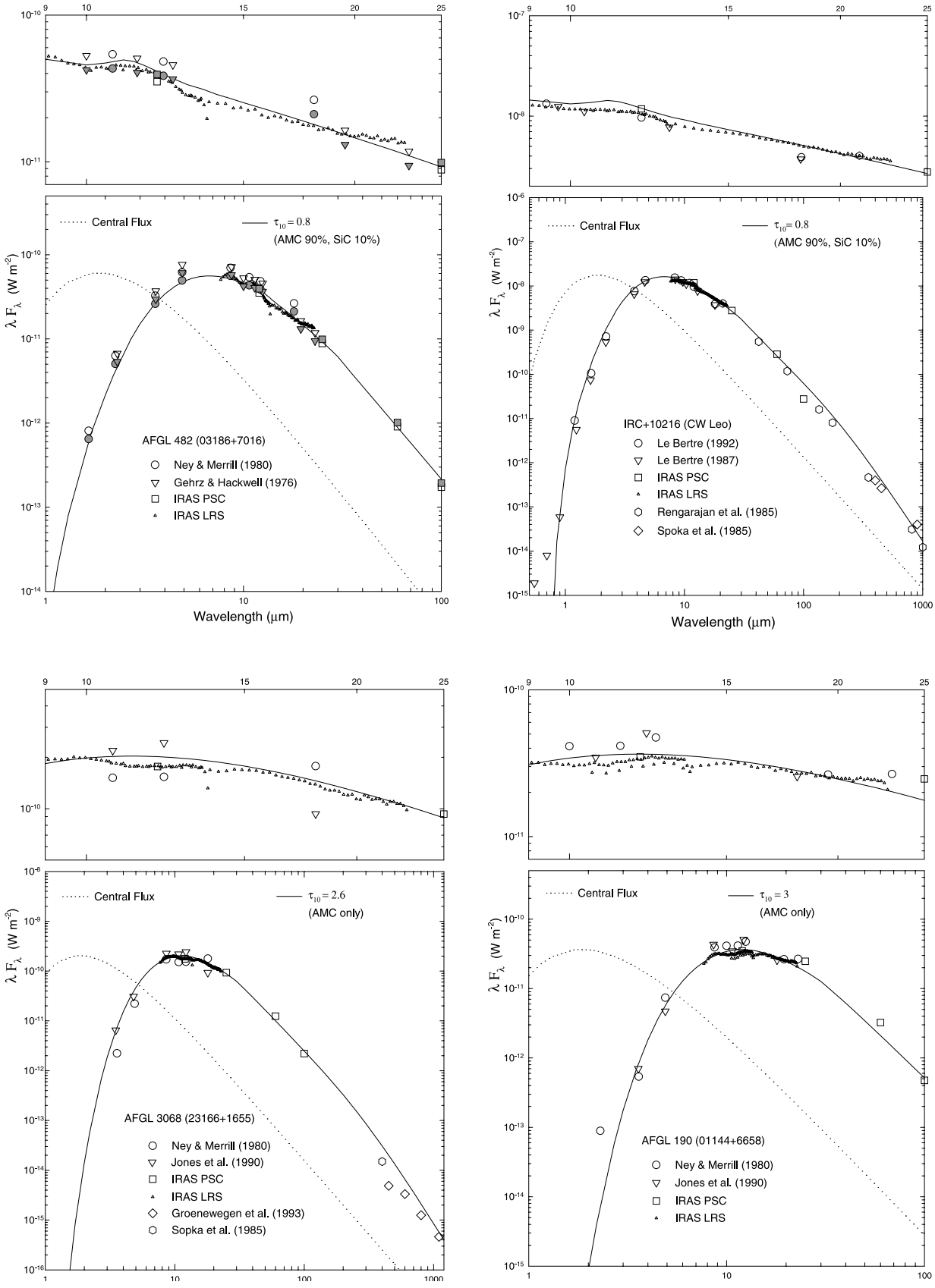

Figure 5 – *continued*

far-infrared fluxes from the *IRAS* PSC and many sources have photometry from the near-infrared to the 10-μm band. Although less useful than a full SED, the large number of observations with less extensive wavelength coverage can be used to form two-colour diagrams that can be compared to our model predictions.

Many investigators have identified hundreds of objects as either optical or infrared carbon stars using various methods. *IRAS* PSC four-colour photometric data are available for many of them. We have collected 40 objects from Rowan-Robinson et al. (1986), 249 objects from Epchtein, Le Bertre & Lepine (1990), 125 objects from Egan & Leung (1991), 28 objects from Volk, Kwok & Langill (1992), 67 objects from Chan (1993), 106 objects from Guglielmo et al. (1993), 28 objects from Volk, Kwok & Woodsworth (1993), 14 objects from Groenewegen (1995), 17 objects from Groenewegen et al. (1995), 20 objects from Guglielmo et al. (1997) and 27 objects from Guglielmo, Le Bertre & Epchitein (1998).

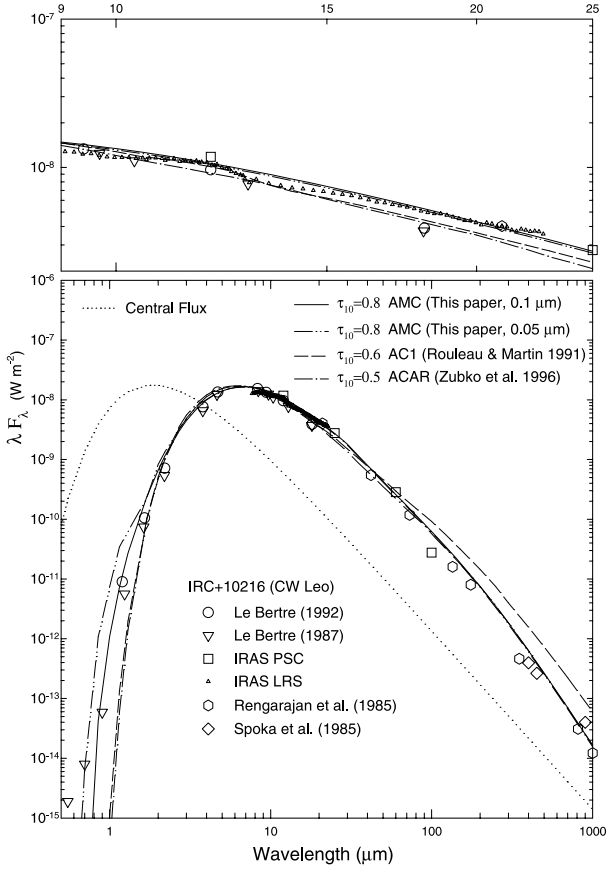

Figure 6. Model results with various opacities of AMC grains compared with the observations of IRC+10216.

Fig. 7 plots the 721 carbon stars in an *IRAS* λF_λ two-colour diagram using [25–60] versus [12–25]. The definitions of [12–25] and [25–60] are given in Guglielmo et al. (1993). Stars with only upper limits at any wavelength were not used. The small open circles are the observational data and the lines with large symbols are the model calculations using various opacity functions for a range in dust shell optical depth ($\tau_{10} = 0.01, 0.1, 1, 2, 3$ and 5). As the optical depth of the dust shell is increased, the [12–25] colour reddens (increases) and the [25–60] colour reddens very slowly.

Carbon stars are distributed along a curve in the shape of a 'C'. A group of stars at the upper-left part are visual carbon stars that show excessive flux at 60 μm which is owing to the remnant of an earlier phase when the star was an oxygen-rich AGB star (e.g. Chan & Kwok 1990). A group of stars at the lower part, which extend to the right-hand side, are infrared carbon stars. The infrared carbon stars at the right part have thick dust shells with large optical depths. The model results using the opacity function obtained in this paper cover the region where most infrared carbon stars are located. Considering the deviations of the observed data points from the model curves, we find that the AMC dust opacity function obtained in this paper fits the observations better than that of previous works. When we add more SiC, the model results deviate more from the cases of AMC only. We use simple mixtures of AMC and SiC grains and this effect is most prominent when the optical depth (τ_{10}) is about 0.1.

Epchtein et al. (1987) used the *K–L* colour and the [12–25] colour to form a two-colour diagram. This diagram proved to be an excellent diagnostic in discriminating between oxygen-rich and carbon-rich stars. Fig. 8 shows this diagram for infrared carbon

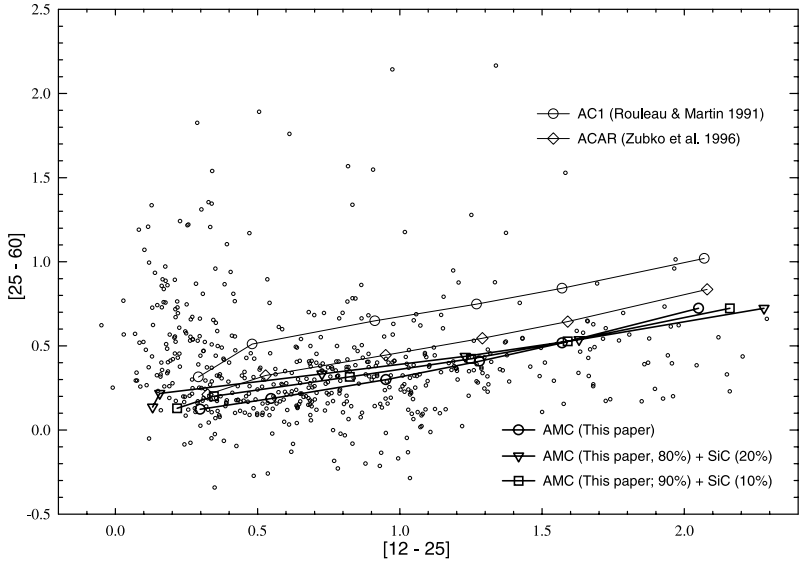

Figure 7. Loci of model results in the *IRAS* two-colour diagram for carbon stars.

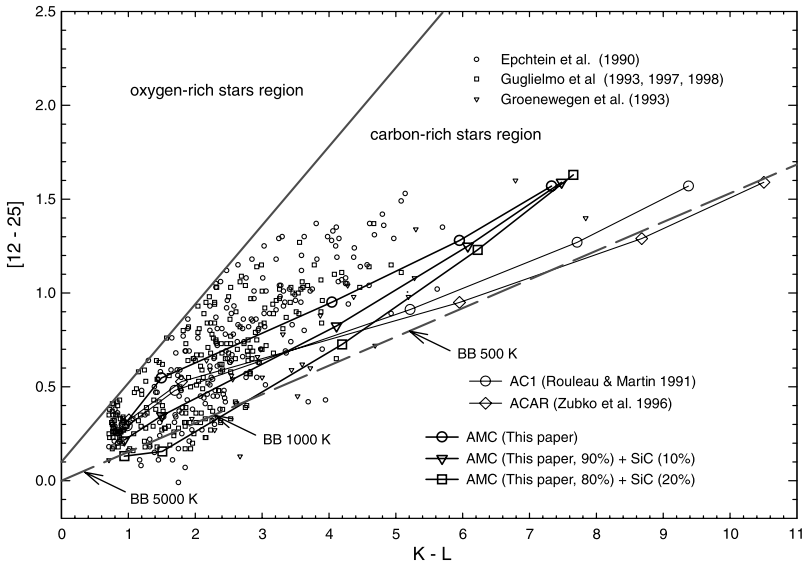

Figure 8. Loci of model results in the [12–25] versus *K*–*L* diagram for infrared carbon stars.

Table 3. Mass loss rates estimated for the models with AMC grains.

τ_{10}	R_c (cm)	$\dot{M}$ ($M_\odot\,yr^{-1}$)
0.01	1.16E+14	3.43E−08
0.1	1.79E+14	5.29E−07
1	2.51E+14	7.42E−06
2	3.02E+14	1.78E−05
3	3.43E+14	3.04E−05
5	4.11E+14	6.07E−05

stars compared with model results. The small symbols are the observational data and the lines with large symbols are the model calculations for a range of dust shell optical depths ($\tau_{10} = 0.01$, 0.1, 1, 2 and 3). In this diagram, the stars in the upper-right region have thick dust shells with large optical depths. The observational data for 249 *IRAS* LRS class 4n objects are compiled by Epchtein et al. (1990) and the data from Guglielmo et al. (1993, 1997, 1998) and Groenewegen, de Jong & Baas (1993) are also shown. The dashed line corresponds to the SEDs of blackbody radiation. The model results using the AMC opacity function obtained in this paper spans the region where most infrared carbon stars are located (near to the middle of the boundaries). When we add more SiC, the model results deviate more from the cases of AMC only. We use simple mixtures of AMC and SiC grains.

We can estimate the mass loss rates for the models presented in the two-colour diagrams. The model results using the AMC opacity obtained in this paper are listed in Table 3. For the central star, the luminosity is taken to be $10^4\,L_\odot$ and the stellar blackbody temperature $T_* = 2000\,K$ is used as discussed in Section 3. We have assumed that the expansion velocity is about $15\,km\,s^{-1}$ for typical carbon stars, the bulk density of an AMC dust grain is $2\,g\,cm^{-3}$, and the dust to gas ratio is 0.0024 (e.g. Blanco et al. 1998). The calculated rates are reasonably in the range of the observed values (e.g. Groenewegen et al. 1998). If we add SiC grains to the opacity, the resulting mass loss rates increase slightly.

Again, note that all the SED models presented in this paper, including the models with other opacity functions, have used the same assumptions of $\rho \propto r^{-2}$, $T_c = 1000\,K$ and $T_* = 2000\,K$. Even though these two-colour diagrams do not reflect the detailed SEDs, we find that the AMC dust opacity function obtained in this paper fits the observations better than in previous works.

6 CONCLUSIONS

We have drawn the following conclusions.

(i) We have investigated the optical properties of the carbon dust grains in the envelopes around carbon-rich AGB stars, paying close attention to the infrared observations of the stars and the laboratory-measured optical data of the candidate dust grain materials. We have compared the radiative transfer model results with the observed SEDs of the stars including the *IRAS* PSC and *IRAS* LRS data.

(ii) AMC dust grains play a major role in producing the overall shape of the SEDs of carbon-rich AGB stars in the wavelength range 1–1000 μm. We have deduced an opacity function of AMC that fits carbon-rich AGB stars well. From the opacity function, we have derived the optical constants of the AMC grains. The optical constants satisfy the Kramers–Kronig relation and produce the opacity function that fits the observations better than previous works. We have used simple mixtures of the AMC and SiC grains for modelling. We have used the optical constants of AMC grains derived in this paper and the optical constants of α SiC grains from Pégourié (1988). We have compared the model results with observations in SED diagrams and infrared two-colour diagrams. We find that the model results fit the observations of infrared carbon stars fairly well in the wavelength range 1–1000 μm for a large sample of objects.

(iii) We have compared the contributions of AMC and SiC grains to the opacity for the cases of simple mixtures of the same size (0.1 μm) spherical grains and spherical core–mantle type grains consisting of an SiC core and an AMC mantle. They have shown different spectral shapes.

(iv) The contribution of AGB stars to the SEDs of galaxies or stellar clusters is believed to be significant (e.g. Bressan, Granato, Silva 1998). To clarify the SED evolution of AGB stars, we need to use the opacity functions of the dust grains that are consistent

with the observations and the physics. If our assumptions of $\rho \propto r^{-2}$ and $T_c = 1000\,\mathrm{K}$ for the dust shells are appropriate, the optical constants of AMC grains derived in this paper and those of silicate grains derived in Paper I would be useful to construct more realistic SED models for the AGB stars in their various stages of evolution.

Note that all the optical data discussed in this paper are accessible through the author's world wide web site `http://ast.chungbuk.ac.kr/~kwsuh/kwsuh.htm`.

ACKNOWLEDGMENTS

I thank the anonymous referee for constructive comments. This work was supported by the Korea Research Foundation Grant.

REFERENCES

Begemann B., Dorschner J., Henning T., Mutschke H., Thamm E., 1994, ApJ, 423, L71
Bergeat J., Sibille F., Lunel M., Lefèvre J., 1976, A&A, 52, 227
Blanco A., Borghesi A., Fonti S., Orofino V., 1998, A&A, 330, 505
Bohren C. F., Huffman D. R., 1983, Absorption and Scattering of Light by Small Particles. Wiley, New York
Borghesi A., Bussoletti E., Colangeli L., 1985, A&A, 142, 225
Bressan A., Granato G. L., Silva L., 1998, A&A, 332, 135
Bussoletti E., Colangeli L., Borghesi A., Orofino V., 1987, A&AS, 70, 257
Chan S. J., 1993, PASP, 105, 1107
Chan S. J., Kwok S. J., 1990, A&A, 237, 354
Egan M. P., Leung C. M., 1991, ApJ, 383, 314
Epchtein N., Le Bertre T., Lepine J. R. D., 1990, A&A, 227, 82
Epchtein N., Le Bertre T., Lepine J. R. D., Marques dos Santos P., Matsuura O. T., Picazzio E., 1987, A&AS, 71, 39
Gauger A., Gail H.-P., Sedlmayr E., 1990, A&A, 235, 245
Gehrz R. D., Hackwell J. A., 1976, ApJ, 206, L161
Gehrz R. D., Ney E. P., Grasdalen G. L., Hackwell J. A., Thronson Jr., H. A., 1984, ApJ, 281, 303
Gezari D. Y., Pitts P. S., Schmitz M., 1998, Catalog of Infrared Observations, 4th edn. NASA Reference Publication 1294
Groenewegen M. A. T., 1995, A&A, 293, 463
Groenewegen M. A. T., 1997, A&A, 317, 503
Groenewegen M. A. T., de Jong T., Baas F., 1993, A&AS, 101, 513
Groenewegen M. A. T., van den Hoek L. B., de Jong T., 1995, A&A, 293, 381
Groenewegen M. A. T., Whitelock P. A., Smith C. H., Kerschbaum F., 1998, MNRAS, 293, 18
Guglielmo F., Le Bertre T., Epchtein N., 1998, A&A, 334, 609
Guglielmo F., Epchtein N., Le Bertre T., Fouque P., Hron J., Kerschbaum F., Lepine J. R. D., 1993, A&AS, 99, 31
Guglielmo F., Epchtein N., Arditti F., Sevre F., 1997, A&AS, 122, 489
Heske A., 1990, A&A, 494, 503
Iben I., 1981, ApJ, 246, 278
Ivezic Z., Elitzur M., 1997, MNRAS, 287, 799
Joint *IRAS* Science Working Group, 1986a, *IRAS* catalogs and atlases, Low Resolution Spectrograph (LRS), A&AS, 65, 607
Joint *IRAS* Science Working Group, 1986b, *IRAS* catalogs and atlases, Point Source Catalog (PSC). US Government Printing Office, Washington DC
Jones T. J., Bryja C. O., Gehrz R. D., Harrison T. E., Johnson J. J., Klebe D. I., Lawrence G. F., 1990, ApJS, 74, 785
Koike C., Hasegawa H., Manabe A., 1980, Ap&SS, 67, 495
Koike C., Kimura S., Kaito C., Suto H., Shibai H., Nagata T., Tanabe T., Sato Y., 1995, ApJ, 446, 902
Kozasa T., Dorschner J., Henning T., Stognienko R., 1996, A&A, 307, 551
Le Bertre T., 1987, A&A, 176, 107
Le Bertre T., 1988, A&A, 190, 79
Le Bertre T., 1992, A&AS, 94, 377
Le Bertre T., 1997, A&A, 324, 1059
Le Bertre T., Gougeon S., Le Sidaner P., 1995, A&A, 299, 791
Lorenz-Martins S., Lefèvre J., 1994, A&A, 291, 831
Ney E. P., Merrill K. M., 1980, Study of Sources in AFGL Rocket Infrared Study. Air Force Geophysical Laboratory, AFGL-TR-80-0050
Noguchi K., Kawara K., Kobayashi Y., Okuda H., Sato S., Oishi M., 1981, PASJ, 33, 373
Omont A. et al., 1995, ApJ, 454, 819
Pégourié B., 1988, A&A, 194, 335
Rengarajan T. N., Fazio G. G., Maxson C. W., Mcbreen B., Serio S., Sciortino S., 1985, ApJ, 289, 630
Rouleau F., Martin P. G., 1991, ApJ, 377, 526
Rowan-Robinson M., Harris S., 1983, MNRAS, 202, 767
Rowan-Robinson M., Lock T. D., Walker D. W., Harris S., 1986, MNRAS, 222, 273
Sopka R. J., Hildebrand R., Jaffe D. T., Gatley I., Roellig T., Werner M., Jura M., Zuckerman B., 1985, ApJ, 294, 242
Speck A. K., Barlow M. J., Skinner A. K., 1997, MNRAS, 288, 431
Speck A. K., Hofmeister A. M., Barlow M. J., 1999, ApJ, 513, L87
Suh K.-W., 1997, MNRAS, 289, 559
Suh K.-W., 1999, MNRAS, 304, 389 (Paper I)
Suh K.-W., Jones T. J., Bowen G. H., 1990, ApJ, 358, 588
Volk K., Kwok S., Langill P. P., 1992, ApJ, 391, 285
Volk K., Kwok S., Woodsworth A. W., 1993, ApJ, 402, 292
Zubko V. G., Mennella V., Colangeli L., Bussoletti E., 1996, MNRAS, 283, 1321

This paper has been typeset from a TEX/LATEX file prepared by the author.